RAPID COMMUNICATION

Raman phonons in multiferroic $FeVO_4$ crystals*

Zhang An-Min(张安民)[a], Liu Kai(刘 凯)[a], Ji Jian-Ting(籍建葶)[a], He Chang-Zhen(何长振)[b], Tian Yong(田 勇)[a], Jin Feng(金 峰)[a], and Zhang Qing-Ming(张清明)[a]†

[a] *Department of Physics, Beijing Key Laboratory of Opto-Electronic Functional Materials and Micro-nano Devices, Renmin University of China, Beijing* 100872, *China*

[b] *State Key Laboratory of Structural Chemistry, Fujian Institute of Research on the Structure of Matter, Chinese Academy of Sciences, Fuzhou* 350002, *China*

(Received 27 September 2015; revised manuscript received 8 October 2015; published online 20 November 2015)

Multiferroic materials are promising candidates for next-generation multi-functional devices, because of the coexistence of multi-orders and the coupling between the orders. $FeVO_4$ has been confirmed to be a multiferroic compound, since it exhibits both ferroelectricity and antiferromagnetic ordering at low temperatures. In this paper, we have performed careful Raman scattering measurements on high-quality $FeVO_4$ single crystals. The compound has a very rich phonon structure due to its low crystal symmetry $(P-1)$ and at least 47 Raman-active phonon modes have been resolved in the low and hightemperature spectra. Most of the observed modes are well assigned with aid of first-principles calculations and symmetry analysis. The present study provides an experimental basis for exploring spin-lattice coupling and the mechanism of multiferroicity in $FeVO_4$

Keywords: Raman scattering, phonon assignment multiferroics

PACS: 63.20.dd, 63.20.dk, 75.85.+t, 78.30.Hv **DOI:** 10.1088/1674-1056/24/12/126301

1. Introduction

The study of multiferroicity is one of the hot frontiers in condensed matter physics. Multiferroic compounds allow the mutual manipulation between magnetism, electricity and strain, and hence are potential materials for next-generation mass-storage and multi-functional devices.[1] Basically most of multiferroic materials can be divided into two categories: one with intrinsic multiferroicity and the other one with improper multiferroicity.[2] Ferroelectricity in the materials with improper multiferroicity can be induced by the orders other than charges. For instance, it has been reported to be originated from spin ordering in $TbMnO_3$,[3] $MnWO_4$,[4] and $Ni_3V_2O_8$.[5] The coupling between magnetism and electricity provides the possibility of the mutual control between the two degrees of freedom. $FeVO_4$ is such a compound with improper multiferroicity. Two antiferromagnetic (AF) transitions at 22 K and 15.6 K, respectively, were observed in poly-crystal $FeVO_4$[6,7] and further confirmed in single crystals.[8] Neutron scattering experiments indicate that a collinear and incommensurate AF order occurs below 22 K while it becomes a non-collinear and incommensurate AF order below 15 K.[9] Ferroelectric polarization was measured in both poly-crystal[9–11] and thin-film[12,13] samples after the second AF transition. In addition, nuclear magnetic resonance (NMR) obtained a Weiss temperature of ∼116 K, indicating a strong spin frustration.[14] The experiments suggest that a magnetoelectric coupling exists in $FeVO_4$.

As one of the fundamental techniques in condensed matter physics, Raman scattering has been widely applied and played a unique role in the studies of multiferroic materials. Raman scattering can be used to probe the lattice distortion which is tightly correlated with ferroelectricity.[12,15] And it is also very sensitive to the magnetoelastic effect and magnetoferroelectricity.[16,17] Doping dependence of magnetoelectric coupling can be characterized by Raman scattering, since it can sensitively catch the information on structural changes. Moreover, as a contactless and non-destructive technique, Raman scattering is particularly useful to the studies of thin films, which are hard to be measured by conventional x-ray diffraction.

In this paper, we have carried out careful Raman scattering measurements on $FeVO_4$ single crystals at low and high temperatures. More than 47 Raman-active modes are observed due to the low crystal symmetry. And we further made a comprehensive assignment of the observed modes by combining with first-principles calculations and symmetry analysis. The

Project supported by the National Basic Research Program of China (Grant No. 2012CB921701), the National Natural Science Foundation of China (Grant Nos. 11174367 and 11004243), the China Postdoctoral Science Foundation, the Fundamental Research Funds for the Central Universities, and the Research Funds of Renmin University of China (Grant Nos. 10XNI038, 14XNLF06, and 14XNLQ03).

†Corresponding author. E-mail: qmzhang@ruc.edu.cn

© 2015 Chinese Physical Society and IOP Publishing Ltd

results are the first step towards the understanding of the mechanism of magnetoelectric coupling in $FeVO_4$.

2. Experiments and methods

$FeVO_4$ single crystals were grown by the flux growth method which has been described elsewhere.[8] Confocal microscopic Raman scattering measurements were carried out with a Jobin Yvon T64000, equipped with liquid-nitrogen-cooled back-illuminated (deep-depletion) charge-coupled device (CCD). A 532-nm diode-pumped solid-state laser (Torus 532, Laser Quantum) was adopted as excitation source. The single crystal used in our measurement is a needle-like sample. The long side along crystalline a axis was defined as x direction. The crystal face $(0,-1,-1)$ is perpendicular to z direction and y direction is determined by the right-hand screw rule. The configuration of backscattering was used and the laser beam was focused on the crystal surface with a spot of 5 $\mu m^2 \sim 10$ μm^2. The laser power was fixed below 1 mW to avoid overheating.

To determine the zone-center phonon modes of $FeVO_4$, first-principles calculations were carried out within the framework of density functional perturbation theory (DFPT)[20] as implemented in the Quantum-Espresso package.[21] The ultrasoft pseudopotentials[22] were used to describe the ion-electron interactions. For the exchange-correlation potential, the generalized gradient approximation (GGA) of Perdew–Burke–Ernzerhof[23] was adopted. After convergence test, the kinetic energy cutoffs of the wave function and the charge density were chosen to be 40 Ry and 400 Ry, respectively. The nonmagnetic electronic structure calculations were performed with a supercell containing 6 Fe atoms, 6 V atoms, and 24 O atoms. For the Brillouin zone sampling, a $2\times2\times2$ k-point mesh was employed. The Gaussian smearing was used around the Fermi surface. In structure optimization, both cell parameters and internal atomic positions were allowed to relax until the forces were smaller than 0.01 eV/Å. Once the equilibrium structure was obtained, the phonon frequencies and displacement patterns were calculated from the dynamic matrix.

3. Results and discussion

The crystal structure of $FeVO_4$ is illustrated in Fig. 1. $FeVO_4$ has a space group of P-1 and all the atoms in its primitive cell occupy 2i positions. Three nonequivalent Fe atoms form two octahedrons of FeO_6 and one polyhedron of FeO_5. Similarly, three vandium atoms are nonequivalent and form three tetrahedrons of VO_4. The polyhedrons are bridged by oxygen atoms located at the vertexes. The point group belongs to C_i and each atom also occupies its space-inversion position. Thus, there are 36 atoms in the primitive cell. In principle this gives 108 vibration modes, among which 54 optical modes are Raman-active A_g modes and 51 optical modes are infrared A_{1u} modes. Such a large amount of Raman-active modes are the natural consequence of the low crystal symmetry.



Fig. 1. (color online) Crystal structure of FeVO4. The structure consists of many polyhedrons of FeO_6, FeO_5, and VO_4 which are connected by sharing the borders and vertexes.

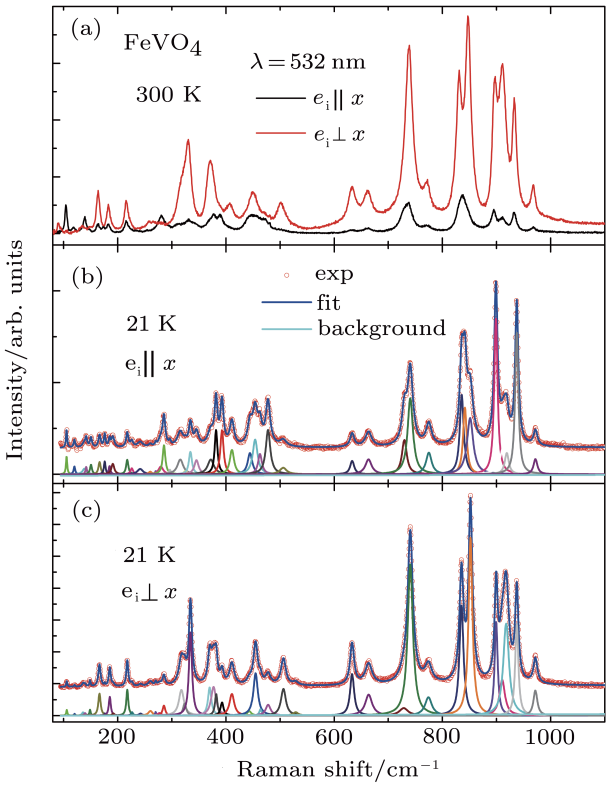


Fig. 2. (color online) Raman spectra collected at different temperatures and configurations. (a) Raman spectra at room temperatures under different configurations. (b) and(c) Raman spectra at low temperatures and the corresponding Lorentzian fitting.

Raman spectra collected at room temperature is shown in Fig. 2(a). The phonon frequency ranges from 90 cm^{-1} to 1000 cm^{-1}. The polarization of incident light is parallel and perpendicular to the long side of the crystal (a axis). The polarized spectra show a strong anisotropy. The intensities under

the parallel configuration are one order of magnitude smaller than those under the perpendicular configuration. This is associated with the orientation of the distorted polyhedron chain, which is almost orthogonal to *a* axis, indicating a quasi-one dimensional structure. It should be noted that the 104 cm^{-1} and 139 cm^{-1} modes appear only under the parallel configuration. This may be related to their special vibration patterns (see below).

The crowd modes at room temperature make it quite hard to distinguish the modes from each other. Thus we further made low-temperature measurements. The low-temperature spectra exhibit a better resolution and allow us to make Lorentzian fitting (Figs. 2(b) and 2(c)). It seems that the fitting works quite well for the low-temperature spectra. 43 and 42 modes are obtained under the parallel and perpendicular configurations, respectively. By comparison of the two configurations, totally 47 modes are resolved in Raman channel. There are 7 Raman-active modes missing in the present spectra. This may be caused by the too low intensities or possible overlapping between so crowd modes. The low crystal symmetry greatly limits the application of symmetry analysis.

The assignment is achieved with the aid of first-principles calculations. The comparison between experimental and calculated mode frequencies is listed in Table 1. The modes in the range of 315 cm^{-1} to 528 cm^{-1} are too close to be reliably distinguished. The frequency difference between two neighboring modes is even smaller than the errors of calculations. They are put together in the table and further assignment of these modes requires more experiments like doping effect, especially isotope doping.

Table 1. The assignment of Raman modes in $FeVO_4$. The modes of No. 1 to No. 18 and No. 42 to No. 54 can be assigned with first-principles calculations, while those of No. 19 to No. 41 are too dense in frequency to be unambiguously assigned at present (see text).

Index	Cal. freq./cm^{-1}	Expt. freq. (21 K)/cm^{-1}	Expt. freq. (300 K)/cm^{-1}	Index	Cal. freq./cm^{-1}	Expt. freq. (21 K)/cm^{-1}	Expt. freq. (300 K)/cm^{-1}
1	91.3	92.13	90.1	28	370.3	410.9871	407
2	102.1	105.9769	103.9	29	378	443.0673	434.5
3	117.9	120.3621	118.09	30	392.6	454.7996	449.08
4	127.7	135.9075	133.9	31	404.2	463.9439	457.8
5	141.6	139.7444	139.43	32	412.7	478.0178	471.7
6	151.5	148.8023	148	33	421.7	506.2249	501.18
7	161.2	166.3215	163.3	34	430.5	528.784	–
8	169.2	176.2091	173.67	35	445.2		
9	175.3	185.3834	182.82	36	454.4		
10	177.4	191.7949	187.7	37	460.1		
11	193.2	217.7747	215.6	38	486.0		
12	209.9	226.4515	223.47	39	495.8		
13	214.7	242.1796	238.4	40	504.7		
14	222.7	260.4192	258.46	41	535.3		
15	250	270.2027	264.88				
16	261.2	277.1371	274.08	42	583.1	633.1113	632.5
17	268.5	285.3859	281.28	43	602.8	663.7241	661.67
18	278.8	296.434	294.45	44	620.3	728.5267	728
				45	675.9	740.6417	738.19
19	296.4	315.6902	311.17	46	726.4	774.1781	771.32
20	304.9	317.7283	314.43	47	741.5	835.2827	830.37
21	311.2	323.6721	317.73	48	750.2	841.5083	837.57
22	323.3	334.486	330.23	49	844.8	851.9171	847.53
23	324.5	345.5894	344	50	849.1	899.3122	894.86
24	335.4	369.9281	367.7	51	855.3	910.4715	906.35
25	338.8	377.098	370.66	52	887.3	917.7792	910.7
26	355.7	382.0173	377	53	909.5	937.4253	932.55
27	364.9	392.7664	390	54	921	971.7895	968.36

Similar to the case of $AlVO_4$,[19] most of the modes in the high-frequency region come from the stretching of V–O–Fe bond. And the low-frequency modes are dominated by the relative torsion motions between the polyhedrons. The modes in the intermediate frequency region are the combination of the low-frequency and high-frequency modes. The vibration patterns of some selected low-frequency torsion modes and high-frequency stretching modes are depicted in Figs. 3(a) and 3(b), respectively. The two modes which only appear under the parallel configuration are still unclear at present and their origins needs to be further studied in experiments and theoretical calculations.

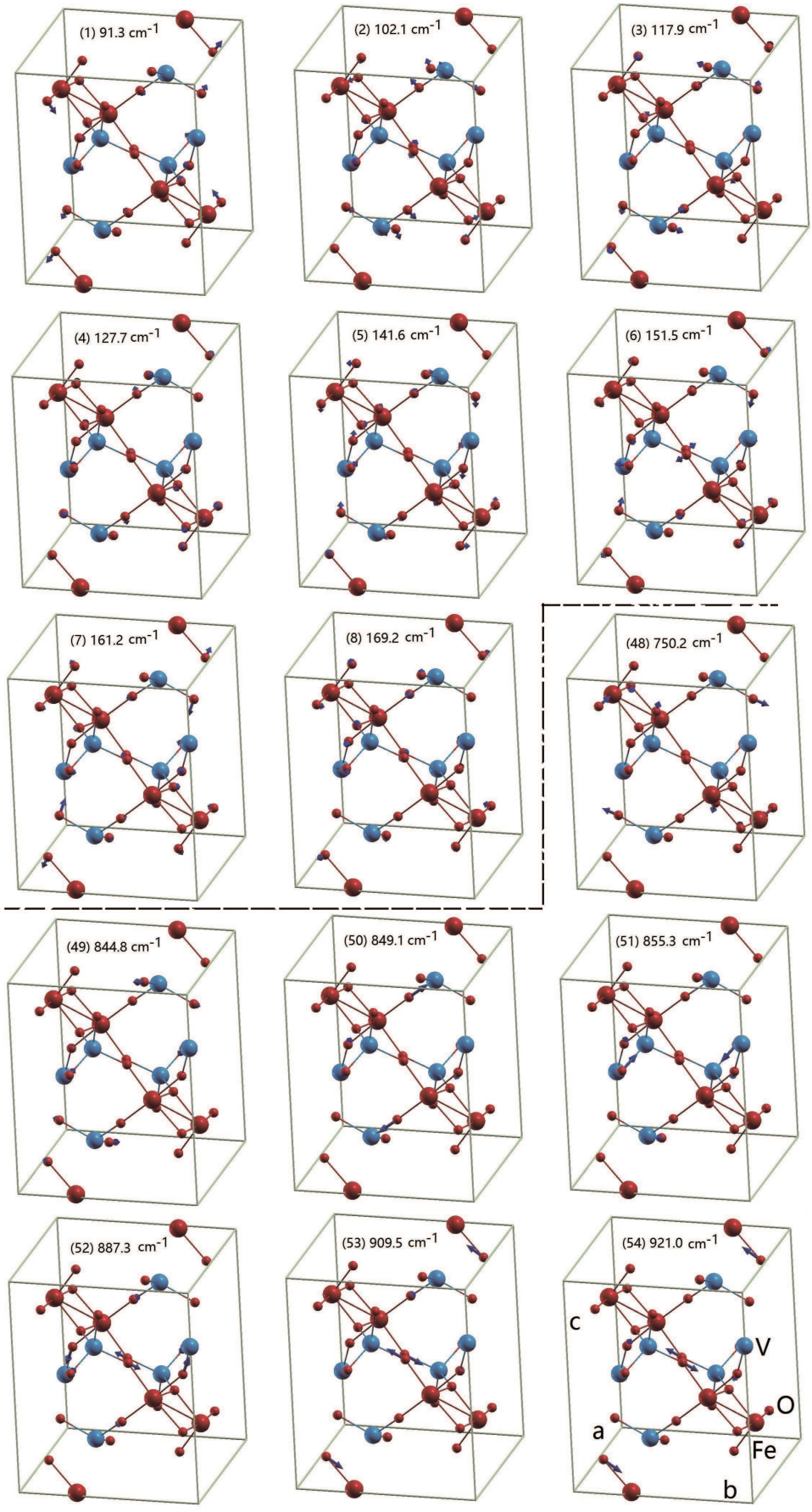


Fig. 3. (color online) Atomic displacement patterns for selected Raman-active A_g modes of $FeVO_4$. The index in each pattern corresponds to that listed in Table 1. 1–8: Bending modes between rigid polyhedron. 48–54: Stretching modes of V–O–Fe bonds.

4. Summary

In summary, we made Raman scattering measurements on single-crystal $FeVO_4$ and resolved at least 47 Raman-active modes. The spectra exhibit a strong anisotropy under two polarization configurations. The spectra can be taken as fingerprints, which are useful to the material synthesis and the studies of doping effect and thin-film samples. The mode assignment has been made by combining first-principles calculations and symmetry analysis. The results provide the fundamental information on lattice dynamics and allow to further explore the ferroelectric transition and magnetoelectric coupling in $FeVO_4$.

References

[1] Gajek M, Bibes M, Fusil S, Bouzehouane K, Fontcuberta J, Barthelemy A and Fert A 2007 *Nat. Mater.* **6** 296

[2] Cheong S W and Mostovoy M 2007 *Nat. Mater.* **6** 13

[3] Kimura T, Goto T, Shintani H, Ishizaka K, Arima T and Tokura Y 2003 *Nature* **426** 55

[4] Taniguchi K, Abe N, Takenobu T, Iwasa Y and Arima T 2006 *Phys. Rev. Lett.* **97** 097203

[5] Lawes G, Harris A B, Kimura T, Rogado N, Cava R J, Aharony A, Entin-Wohlman O, Yildrim T, Kenzelmann M, Broholm C and Ramirez A P 2005 *Phys. Rev. Lett.* **95** 087205

[6] Levinson L M and Wanklyn B M 1971 *J. Solid State Chem.* **3** 131

[7] Surikov V I, Lisson V N, Surikov V I and Kourov N I 1983 *Fizika Nizkikh Temperatur (Kiev)* **9** 1109

[8] He Z, Yamaura J I and Ueda Y 2008 *J. Solid State Chem.* **181** 2346

[9] Daoud-Aladine A, Kundys B, Martin C, Radaelli P G, Brown P J, Simon C and Chapon L C 2009 *Phys. Rev. B* **80** 220402

[10] Kundys B, Martin C and Simon C 2009 *Phys. Rev. B* **80** 172103

[11] Zhao L, Wu M P Y, Yeh K W and Wu M K 2011 *Solid State Commun.* **151** 1728

[12] Dixit A and Lawes G 2009 *J. Phys.: Condens. Matter* **21** 456003

[13] Dixit A, Lawes G and Harris A B 2010 *Phys. Rev. B* **82** 024430

[14] Zhang J, Ma L, Dai J, Zhang Y P, He Z, Normand B and Yu W 2014 *Phys. Rev. B* **89** 174412

[15] Iliev M N, Abrashev M V, Laverdiere J, Jandl S, Gospodinov M M, Wang Y Q and Sun Y Y 2006 *Phys. Rev. B* **73** 064302

[16] Jia C, Onoda S, Nagaosa N and Han J H 2007 *Phys. Rev. B* **76** 144424

[17] Choi Y J, Yi H T, Lee S, Huang Q, Kiryukhin V and Cheong S W 2008 *Phys. Rev. Lett.* **100** 047601

[18] Kumarasiri A, Abdelhamid E, Dixit A and Lawes G 2015 *Phys. Rev. B* **91** 014420

[19] Brázdová V, Ganduglia-Pirovano M V and Sauer J 2005 *J. Phys. Chem. B* **109** 394

[20] Baroni S, de Gironcoli S, Dal Corso A and Giannozzi P 2001 *Rev. Mod. Phys.* **73** 5159

[21] Giannozzi P *et al.* 2009 *J. Phys.: Condens. Matter* **21** 395502

[22] Vanderbilt D 1990 *Phys. Rev. B* **41** 7892

[23] Perdew J P, Burke K and Ernzerhof M 1996 *Phys. Rev. Lett.* **77** 3865